Elias Lewi and Erwin Groten

Spatial variation of time lag between SSTA and LOD

Es werden neue, vertiefte Untersuchungen über die zeitlichen und regionalen Zusammenhänge zwischen der Erdrotation (LOD) und der Meeresoberflächentemperatur (SSTA) vorgestellt.

Introduction

Due to the advances in both space geodetic measurement and weather monitoring systems, the interaction of El Niño-/Southern Oscillation (ENSO) to the variations in the Length of Day (here after will be referred as LOD) has been closely monitored and intensively studied by many researchers during the last two decades. At present it is even possible to model the events of ENSO (e.g., Suarez and Schopf, 1988; Stockdale et al., 1998; Delecluse, et al., 1998; Dijkstra and Burgers, 2002) and even attempts are made to predict it few months ahead (e.g., Latif, et.al., 1998; Tang and Kleeman, 2002; Collins, et al., 2002; Clarke and Van Gorder, 2003; Zhang et al., 2003).

One can classify any studies on the interdependence between ENSO and LOD in two categories. The first one is the analysis of the existence of any interaction between LOD and ENSO and the modeling of this interaction. Then the next step will be the prediction of the future incidents based on the models available. Though a lot has been done in the first category (e.g., Stefanick, 1982; Rosen, et al., 1984; Eubanks, et al., 1986; Chao, 1988; Dickey, et al., 1994; Groten, et al., 2000; Yan, et al., 2002), the prediction part is not yet studied well. One of the main reasons for this would be the non-availability of a well developed and widely acceptable prediction method for ENSO.

Therefore, the task ahead is first to establish and quantify the correlation between ENSO and variations in earth rotation parameters and then establish a model that can be used in predicting the effect of one on the other. In this paper we present a study made to analyze the spatial dependence of the time lag of variations in LOD to ENSO events.

Data and Data processing

The LOD data used in this work is that from the International Earth Rotation and Reference Systems Service (IERS), smoothed values of Earth Orientation Parameters (EOP) at 1-day intervals (C04). On the other hand, the Sea Surface Temperatures (SST) data is taken from the National Climate Data Center (NCDC). The Extended Reconstructed Sea Surface Temperatures, version 2 (ERSST.v2) data from January 1854 to June 2004 has been used to characterize ENSO.

Since the available LOD data set begins at 1962, the SST data has been windowed for the time beginning January 1962 to July 2004. Using this data set an average value has been computed for each month separately, over the base time 1963 to 2003. Then, the Sea Surface Temperature Anomaly (SSTA) is computed by removing this mean value for each station from the raw data. The resulting SSTA anomaly is given together with ENSO events (CPC, 2004) in Figure (1a). The occurrences of El Niño and La Niña are marked red and blue respectively. Moreover, since the SST data is available at one month

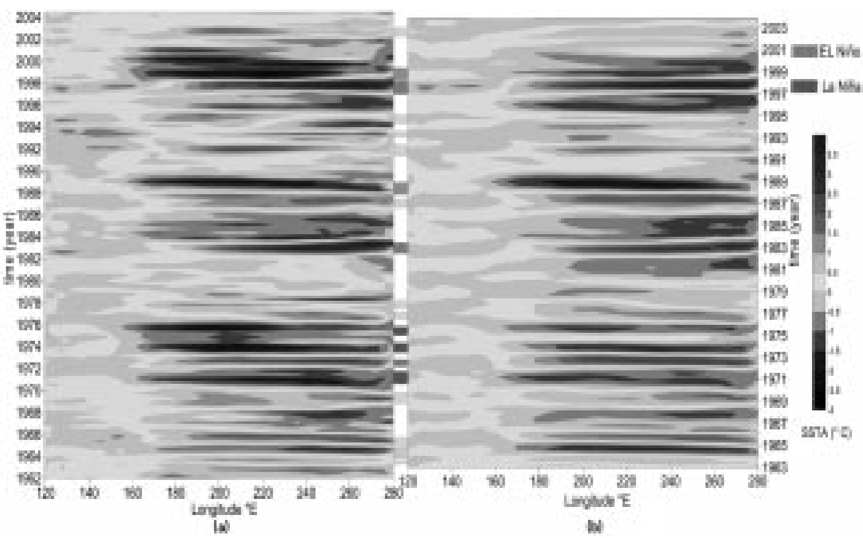

Fig. 1: Time and spatial variation of (a) SSTA and (b) filtered SSTA together with the occurrences of El Niño and La Niña, at latitude 2° south.

interval the LOD data set is also averaged for each month (Figure 2a).

One way of studying the variations on Earth Rotation Parameters (ERP), due to changes in the climate, is by using excitation functions from the latter (e.g., Johnson et al., 1999) and compare them with observed ERP. This is a common practice both for low (e.g., Dickey et al., 1994) and high frequency (e.g., Gross, 2000) analysis. Others use ENSO indices developed using different methods and data sources (e.g., Chao, 1988) and compare it with the LOD. However, here it is preferred to use the SSTA data directly to be able to study the variations both in space and time.

A choice of the 2° south latitude, from 120°E to 180°E, is made after a careful and systematic analysis of the peak of the SSTA anomalies.

Since our interest lies in the inter-annual correlations caused by signals with periods between 1.3 to 10 years, it was necessary to remove other known effects that lie out of this range, using a least squares fit to periodic functions. This method of removing undesired frequencies is preferred after testing a number of band-pass, low pass and high pass filters, that have affected the time lag. The removal of frequencies is strictly limited to known effects (e.g., McCarthy and Petit, 2004, pages 93-94; Abarca del Rio et.al. 2003; Jochmann and Greiner-Mai, 1996).

After removing these selected frequencies, as the last step of the filtering process, very short wave length (below 7 months) effects are smoothed using the Savitzky-Golay smoothing filter (Press, et al. 2002), that is well suited for the preservation of the first moment, which is the mean position in time. A window of 7 months (three data points to the left and right from the point of interest), with 2nd degree has been used. This choice is made by keeping in mind the weakness of the Savitzky-Golay smoothing filter that broadens the width of the high frequency signal when used with lower degree. However, through this choice it has been observed that it is not only the first moment but also the higher moments of the periods greater than 8 months are left intact. The resulting filtered SSTA data is presented in Figure (1b), while the LOD data is presented in Figure (2b) together with El Niño event (CPC, 2004 and IRI, 2004).

Methods

The correlation between the series is considered to be linear, though it is known that the oceanic and atmospheric system is non-linear, and the Pearson correlation coefficient is computed to study the interaction between them. By definition the Pearson correlation coefficient between two series x and y, at a time lag of τ, is computed as $r(\tau)$, using

$$r(\tau) = \frac{\sum_i [x(i) - \bar{x}]*[y(i+\tau) - \bar{y}]}{\sqrt{\sum_i [x(i) - \bar{x}]^2}*\sqrt{\sum_i [y(i+\tau) - \bar{y}]^2}} \quad (1)$$

Here $\bar{x}$ and $\bar{y}$ are means of the corresponding series x and y, with i = 1,2, …, N being the ith data point in each series and N is the total number of data points. It should be kept in mind that for the SST data set the mean is already removed. It is assumed that the data is cyclic and hence data wrapping has been applied. This way we produce a

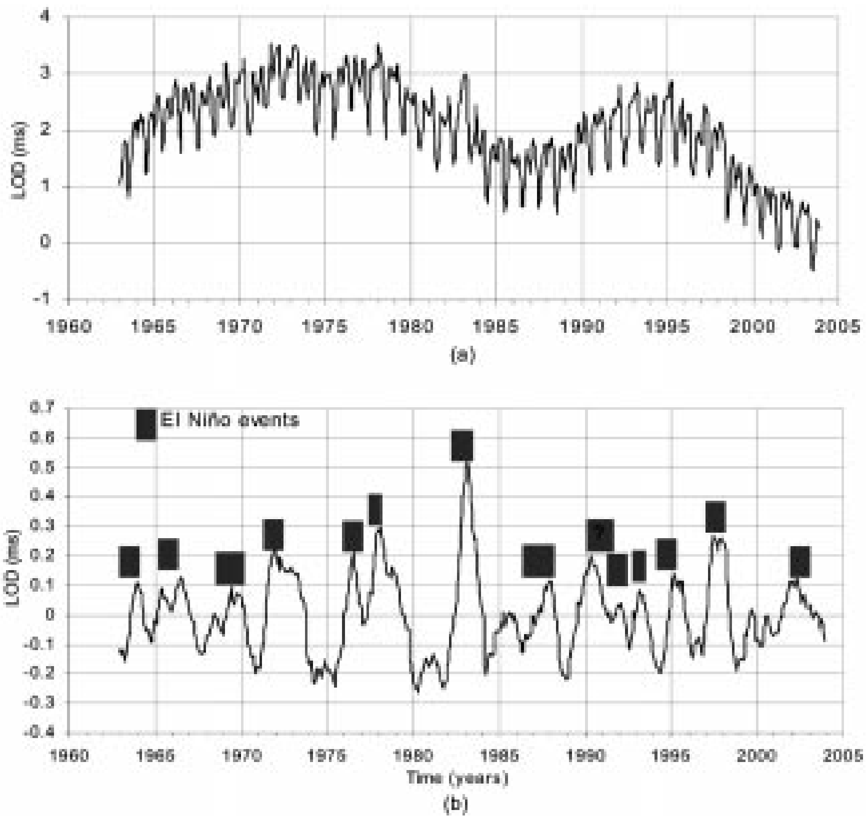

Fig. 2: The LOD data series that is used for the analysis (a) raw data (b) filtered data, together with El Niño events.

negative time lag data set, using those time lags greater than the mid data point.

To ascertain the significance of the linear correlation coefficient, a t-test has been carried out. Here the null hypothesis is that there is no linear dependence between the two series, i.e r = 0. Equation (2) is used to compute the t values.

$$t = \sqrt{\frac{r^2 \nu}{1 - r^2}}, \tag{2}$$

where $\nu = N-2$ is the degree of freedom. Then the probability $A(t/\nu)$, for ν degrees of freedom, that the test statistic t would be more extreme than the one obtained from equation (2), is computed using

$$A(t/\nu) = \frac{1}{\nu^{1/2}\beta(1/2, \nu/2)} \int_{-t}^{t} (1 + x^2/\nu)^{-\frac{\nu+1}{2}} dx. \tag{3}$$

Here $\beta(1/2,\nu/2)$ is the Beta function. Details can be found in Press et al. (2002). Small value of $A(t/\nu)$ in equation (3) casts doubt on the truthfulness of the null hypothesis and hence its rejection or, in other words, proves the significance of the correlation.

It is also a common practice to counter check the results found in the time domain and analyze it deeper in the frequency domain, through the use of coherence analysis. The usage of the coherence analysis will not only allow to study the correlation and time lag between ENSO and LOD, but also analyzes which frequency bands are responsible for the correlation at a given phase lag. For any two random time series x(t) and y(t), with power spectra of $S_{xx}(\omega)$ and $S_{yy}(\omega)$ respectively and cross power spectrum $S_{xy}(\omega)$, the complex coherence function $C_{xy}(\omega)$ is computed using

$$C_{xy}(\omega) = \frac{S_{xy}(\omega)}{\sqrt{S_{xx}(\omega) S_{yy}(\omega)}}. \tag{4}$$

Here ω is the angular frequency. Since $S_{xx}(\omega)$ and $S_{yy}(\omega)$ are real quantities and $S_{xy}(\omega)$ is complex, it automatically follows that $C_{xy}(\omega)$ will be a complex quantity with magnitude and argument. The magnitude $(0 < \gamma(\omega) < 1)$ is called the coefficient of coherence (Foster and Guinzy, 1967) and the argument $(-\pi < \varphi(\omega) < \pi)$ the phase lag. Essentially, γ is the average, normalized amplitude of the cross power spectrum. It is the measure of how good the two time series are correlated. It is mathematically analogous to the Pearson product moment correlation given in equation (1). The square of $\gamma(\omega)$ (equation 5) is the squared coherence spectrum, which also satisfies the inequality $0 < \gamma^2(\omega) < 1$ (Jenkins and Watts, 1968). In some literature the square coherence is referred to as the coherence function (e.g., Otens and Loren, 1972). In this paper we preferred to call $C_{xy}(\omega)$ in equation (4) as the complex coherence function, its magnitude $|C_{xy}(\omega)|$ the coefficient of coherence and $\gamma^2(\omega)$ in equation (5) as squared coherence spectrum.

$$\gamma^2(\omega) = |C_{xy}(\omega)|^2 = \frac{|S_{xy}(\omega)|^2}{S_{xx}(\omega) S_{yy}(\omega)} \tag{5}$$

The direct application of equation (5) on linearly dependent data will give unity at all frequencies, irrespective of what the true values are. To overcome this problem one can either average $S_{xx}(\omega)$, $S_{yy}(\omega)$ and $S_{xy}(\omega)$ over adjacent frequencies or average the replications of data at a given frequency, from different realizations, or combine both approaches. In this work, both approaches are used together. Actually, by averaging the power spectrum based on sampled data we are trying to approximate equation (5) and hence, in practice, we are computing the squared sample coherence $\gamma^2(\omega)$. However, for the purpose of simplicity we will refer to this quantity as squared coherence. Since the process of averaging stabilizes the coherence value but degrades the spectral resolution the choice of the windows has been done carefully not to loose too much resolution.

The replication of data at a given frequency is usually attained by dividing each data set into k blocks and compute $S^j_{xx}(\omega)$, $S^j_{yy}(\omega)$ and $S^j_{xy}(\omega)$, for j = 1,2,...,k. Here we have used the Welch Modified Periodogram method (Welch, 1967; Rabiner and Gold, 1975) to generate the different blocks. In this method, any two series (in our case SSTA and LOD) will be segmented into k blocks, with the same amount of data that have overlapping data points. Then the mean values $\hat{S}_{xx}$, $\hat{S}_{yy}$ and $\hat{S}_{xy}$, at the frequency ω, are obtained by averaging the data from the k blocks. Using these averaged power and cross power spectral densities, spectral averaging over adjacent m discrete frequencies has been carried out by averaging the cross- and power spectrums within the given frequency window. The coherence value achieved using the above procedure should be judged for its reliability, so that it can be accepted as a reasonable estimate. For this the measure given in equation (6) has been used (Brillinger 1975, page 334).

$$c^2 = 1 - \alpha^{1/(n-1)} \tag{6}$$

where $\alpha = 1-p$ and p*100% is the confidence threshold. In some literature (e.g., Thompson 1979) equation (6) is used with n = k, where k is again the number of realizations or the number of data blocks. Others (e.g., Chao 1988) use n = m, which is the number of elementary Fourier bandwidth, where spectral averaging is conducted. Here we used equation (6) with n = k + m, where m and k have the same previous meanings.

To compute the time lag from the phase angle, which is the argument of equation (4), first a straight line is fitted to the computed phase within a selected window, using the robust estimation technique. Then, this line is considered to be the best estimate to the ideal phase and the time lag $\tau(\omega)$ is computed using this phase estimate. For the purpose of comparison a least squares fit has also been tested.

Results and discussions

A visual judgment will affirm that the filtered LOD data (Fig. 2b) has clearly exhibited all ENSO events perfectly, except some minor differences. For example, the 1973 anomaly is wider than the SSTA during the same period.

We have also observed this in some previous work (e.g., Chao, 1988). The other area where we observed a mismatch is the peak value at 1990. This peak is not depicted at all longitudes of the SSTA. It has exhibited itself only between longitudes 215°E and 240°E and that also with a very weak signal. This event is also not mentioned in the CPC (2004) list of ENSO events, which is based on SSTA. However, in the IRI (2004) list, which is based on Southern Oscillation index (SOI), it is given as ENSO event. Though, the filtered LOD data shows a strong peak at this position and the IRI included it as ENSO event, since it is not generally accepted with certainty, it has been marked with question mark in Fig. (2b). In contrast, the 1991 – 92 event is relatively weaker in the LOD data, than what has been observed in the SSTA.

It is also notable that there are some high frequency effects that are still present in the data. This is because the contributions of ocean, atmosphere and hydrological phenomena in the annual and semi-annual periods have variation in their amplitude, phase and periods (Höpfner, 1996 and 2001). The complete removal of this remnant minor frequencies would have been possible using a lower degree Savitzky-Golay smoothing filter and by broadening the width of the window. But, this will be at the risk of loosing some energy from periods that are above one year. In this work, the selection of the width and degree of the Savitzky-Golay smoothing filter is done by observing the power spectrum of both data sets and it has been made sure that energies from periods more than one year are kept untouched by the filter. From the 511 data points only 492, i.e. 1963 to 2004, are used to reduce the effects of filtering at the end points, which actually, at the worst demands only 3 months from each side.

The correlation of the time variation of the filtered SSTA, at each longitude, with the filtered LOD data is carried out using equation (1). Taking that the data is cyclic, data wrapping has been used. Fig. (3) shows the maximum correlations at each longitude together with the time lag (τ) at which the maximum correlation has occurred. All values lie above the 99% confidence level except at those longitudes between the two vertical gray lines. It is only at longitude 160°E that the confidence level fall bellow 95%. Considering the 492 data points taken for the computation, it will not be a surprise to get a 99% confidence threshold even for the 0.15 correlation coefficient. The maximum correlation coefficient found is 0.61 at 272°E. The maximum correlation at each longitude could have been improved by removing periods above 1.3 years or by increasing the window size of the Savitzky-Golay smoothing filter. However, we have preferred not to surpass the1.3 years period so that any energy originating from periods above 1.3 years will be available in its entirety for the analysis.

It is interesting to note that the time lag is inconsistent throughout the area. If one considers the area where the correlation coefficient attains an average value of 0.58 (174°E to 178°E) one can see that the LOD data has no time lag with the SSTA data. As we move eastward, the time lag increases to two months lead between 218°E and 234°E and again to no time lag at 276°E. This will be reversed further eastward starting 178°E where the LOD data has a time lead. In the western

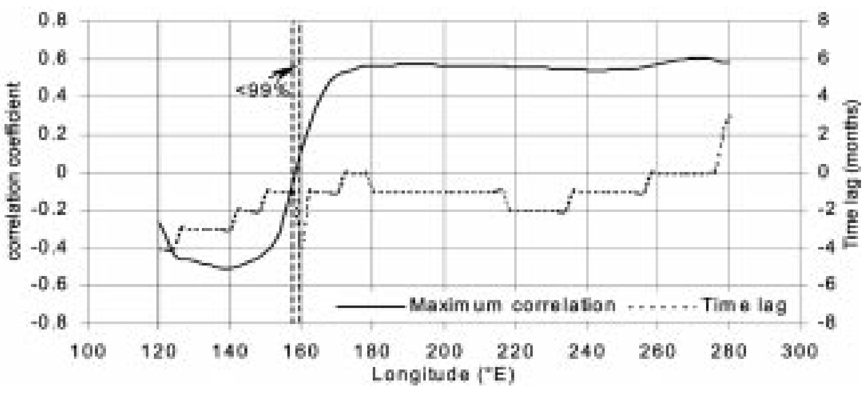

Fig. 3: Maximum Linear correlation of filtered SSTA with filtered LOD data at different longitudes and the time lag (τ) at which these maxima are occurring.

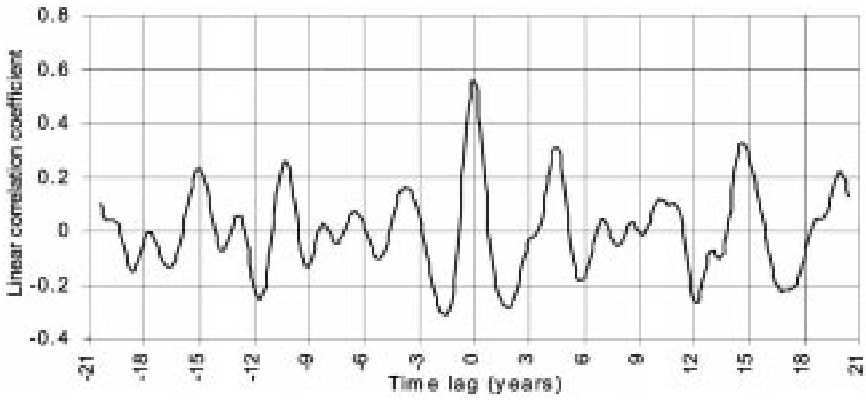

Fig. 4: The linear correlation of filtered SSTA with filtered LOD at different time lag (τ).

part of Pacific there is a maximum correlation coefficient of – 0.51 at 140°E. The axis of reversal, from the negative to positive correlation, is at 160°E. Henceforth, for the sake of simplicity, we call the area west of this axis the Western Pacific and that towards east the Eastern Pacific. Fig. (4), which shows the variation of the correlation coefficient with time lag at 160°E, demonstrates a typical behavior for the Eastern Pacific area. The Figure depicts a quasi-periodic behavior with an average period of 3.6 years. This period is specially to be noticed in the negative axis of the time lag. Of course, it is superimposed by the 5 year and 2.5 year periods.

To deeply analyze the results achieved in the time domain we have carried out some spectral analysis by computing the complex coherence function which is given in equation (4). We used a rectangular window to transfer the data to the frequency domain. It would have been also possible to use non-rectangular windows in the time domain, before transforming the data to the frequency domain. Though, this would have reduced spectral leakage, it was at the cost of degrading the resolution.

Then to make use of the Welch modified periodogram we took a block of L = 256 data points with a shift D = 59 (Welch, 1967) and made sure that there is a 75% data overlap to form k = 5 blocks. Then the resulting averages from the 5 blocks, at each frequencies, are again averaged over the neighboring frequencies using an m = 3 months window. A sound resolution and interpretable solutions are found when the sum of k and m is between 5 and 10.

Here, it should be noted that because of the introduction of an overlapping data window the data sets would not be independent. Therefore, the usage of equation (6) might be wrong and hence we have applied the correction factor $k_{new} = 9k/11$, suggested by Welch (1967) before using it in equation (6).

The squared coherence and the phase are then computed from the complex coherence function. To demonstrate the result we have taken again the longitude 160° 1E. As one can see from Fig. (5a) there is a 0.8 squared coherence value, at the frequency 0.281 cycles/year (a period of 3.55 years), which is also the strongest quasi-period in the SSTA. This squared coherence value is well over the 99% confidence threshold. This is attributed to the optimal choice of k and m values that are taken for the analysis.

In the high frequency range, there is also a strong coherence, at the period of 5 to 5.4 cycles/year. We consider this coherence as insignificant for this study, because the energy, in this frequency range, is in the order of 10^{-7} when compared to the energy in the 0.281 cycles/year. It should be noted that a complete removal of frequencies in a given band from both signal, which amounts to a very small flat spectrum, will also lead to a coherence value of 1. The smaller coherences that are seen in the semi-annual and about 1/3 year are not that much significant and might be due to remnant signals from different causes, in this frequency band, that are hard to completely remove because of variations in amplitude and phase.

The phase lag, which is given in Fig. (5b), clearly shows that there is a complete shift in the trend of the phase at about 1.55 cycles/year. This clearly shows that the Savitzky-Golay smoothing filter didn't affect the long wavelengths that are above 8 months. The approximation to the computed phase, using the robust estimation technique, is done for frequency window between 0.098 and 0.8 cycles/years, where no filtering is applied. In the curve fitting procedure robust estimation technique is more stable than the least squares method, which is very sensitive to the change of the window size. This is also an expected result. The fitted phase has given a good estimate of the ideal linear phase caused by the one-month time lag

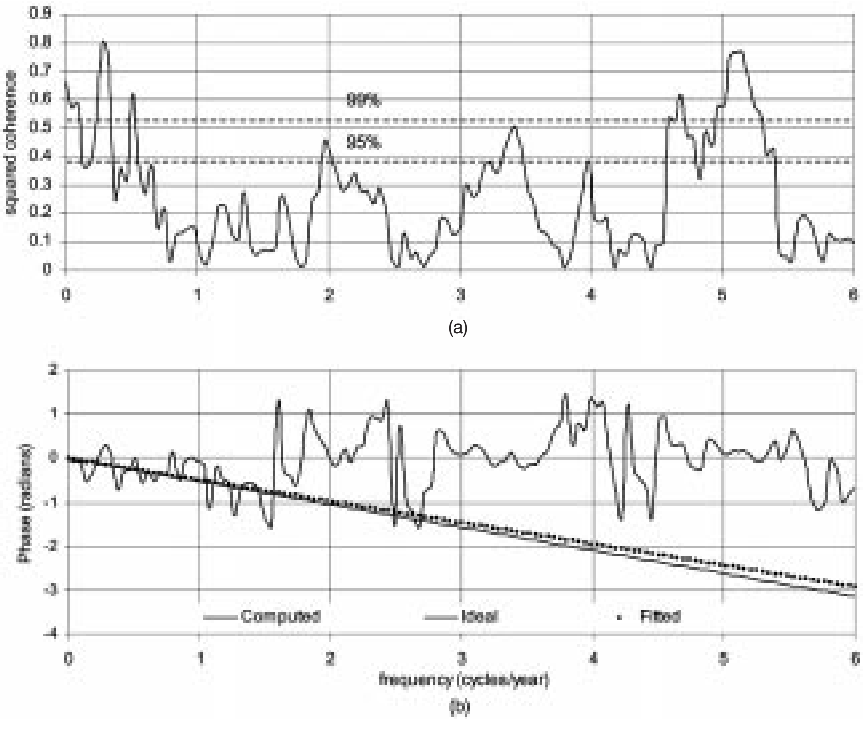

Fig. 5: The full spectrum, complex coherence function between filtered SSTA and LOD. (a) Squared coherences with dotted lines showing the 95% and 99% confidence threshold. (b) Phase, a linear fit to a selected window of the phase and an ideal one-month linear phase.

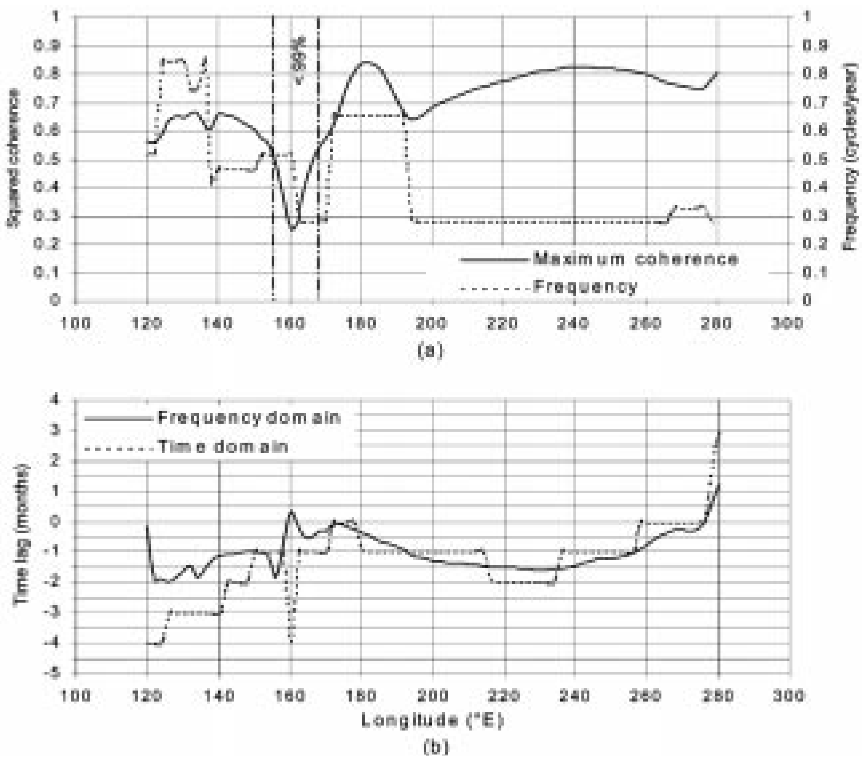

Fig, 6: Result of the coherence analysis (a) Maximum squared coherence and the frequency band at which it occurs (b) The comparison of the time lag obtained from the coherence analysis and correlation analysis.

that was found in the time domain analysis. The same analysis was also carried out parallel at the other longitudes, using the same parameters. The maximum coherence at each longitude is given in Fig. (6a). As one can see from the Figure all points are above the confidence threshold, but those between 156°E and 166°E. The comparison of this result with the one from the time domain shows, that the confidence threshold chosen for the coherence analysis has rejected more points, east of 160°E. Moreover, the doted curve in Fig. (6a) clearly showed that in all the profiles east of 196°E the energy from the frequency band about 0.281 cycles/year is the main cause of the correlation between LOD and SSTA. The term band is used deliberately to emphasize that the results are based on spectral averaging.
The comparison of the time lags at each longitude (Fig. 6b), where maximum correlations and coherences occur, showed a notable result. In most of the data points LOD lags behind SSTA. Because of the one-month resolution of the data, the time lag in the time domain changes stepwise. In contrary, the one from the frequency domain showed a smooth change. As an example, at 118°E the time lag from the coherence analysis has crossed the – 1.5 months line. This is rounded off to 2 months in the time lag from the correlation analysis. Except for the small area at about 260°E this holds true for the area between 180°E to 276°E.
The spatial variation of the time lag is the result of the development of the SSTA in the area. The development of the SSTA followed from the 1983 event, which is also the biggest anomaly in the filtered LOD data, showed that the temperature starts to accumulate at about 130°E and propagate in both east and west directions. Sea level changes (Cardon et al., 1998) also show the same phenomena during the 1997 – 1998 El Niño event. However, this is not checked for non-major events. From the result of the time lag analysis and from the 1983 event which is analyzed thoroughly, we found that the zero time lag is during the time, when ENSO event covered the whole eastern Pacific ocean, just before the subsidence of the accumulated temperature. The time lead of LOD data at about 180°E is because the SSTA stays longer in this area before it subsides.

Conclusion

The filtering of the LOD and SSTA by selectively removing undesired frequencies from the signal is found to have a big advantage in not altering the time lag. In our study the removal of undesired signal using periodic function yields a very good result, which is also in agreement with previous work (e.g., Chao, 1988). Complete removal of semi-annual periods was not possible due to strong variation in their amplitude, phase and periods. However, the energy from these bands has been reduced to minimal level that it doesn't affect our interpretation. The usage of the Savitzky-Golay smoothing filter gave a very good result in suppressing remaining energies from this and higher frequency bands.
The filtered LOD data has exhibited all ENSO events. The 1990 event, which is not considered as El Niño event in the analysis based on SSTA, is seen in our data and it agrees with El Niño events that are based on SOI.
The method we implemented here in computing the time lag from the phase in the frequency domain produced a remarkable result. The time and frequency domain analysis showed that the time lag varies spatially. Most of the previous work, in studying the correlation of ENSO to LOD made use of the SOI. We have shown here that such an approach might only lead to partial understanding

of complex phenomena. Therefore, future studies should also take the spatial dimension into consideration. A better approach would be to analyze the angular momentum derived from the climate data that describe ENSO effects. It has been also noted that the main correlation between SSTA and LOD is coming from the energy in the 0.281 cycles/year frequency band, which is also the dominant quasi-periodic frequency in SSTA.

Because of the quasi-periodic nature of the ENSO events, it will be encouraging to repeat the analysis discussed in this paper using the Wavelet method, to further analyze time dependency.

Acknowledgement

The German Research Foundation (DFG) has sponsored this study. The financial support is well appreciated. Data are used from the International Earth Rotation and Reference Systems Service (IERS) and National Climate Data Center (NCDC).

References

[1] Abarca del Rio, R., Gambis, D. Salstein, D., Nelson, P., Dai, A.: 2003, Solar activity and earth rotation variability, Journal of Geodynamics, Vol. 36, 423–443.

[2] Brillinger, D. R., 1975, Time series: Data Analysis and Theory, Holt, Rinehart and Winston, Inc. New York, USA.

[3] Cardon, K., Goryl, P., Scharro, R., Benoeniste, J.: 1998, El Niño Observed by ERS, Earth observation Quarterly, No. 59, June 1998, ESA.

[4] Chao, B. F.: 1988, Correlation of Inter-annual Length-of-Day Variation with El Niño/Southern Oscillation, 1972–1986, Journal of Geophysical Research, Vol. 93. No. B7, 7709–7715.

[5] Collins, M., Frame, D., Sinha, B., Wilson, C.: 2002, How far ahead could we predict El Niño, Geophysical Research Letters, Vol. 29, No. 10, 130-1–130-4.

[6] Clarke, A. J., Van Gorder, S.: 2003, Improving El Niño prediction using a space-time integration of Indo-Pacific winds and equatorial Pacific upper ocean heat content, Geophysical Research Letters, Vol. 30, No. 7., 52-1–52-4.

[7] CPC, 2004 (reference year), Cold & Warm episodes by season, http://www.cpc. ncep.noaa.gov/ products/analysis_monitoring/ensostuff/ensoyears.html, Home page of the National Oceanic and Atmospheric Administration, National weather service, Climate prediction Center, USA.

[8] Delecluse, P., Davey, M. K., Kitamura, Y., Philander, S. G. H., Suarez, M., Bengtsson, L.: 1998, Coupled general circulation modeling of tropical Pacific, Journal of Geophysical Research, Vol. 103, No. C7, 14,357-14,373.

[9] Dickey, J. O, Marcus, S. L., Hide, R., Eubanks, T. M., Boggs, D. H., 1994, Angular momentum exchange among the solid Earth, atmosphere, and Ocean: A case study of the 1982–1983 El Niño event, 1994, Journal of Geophysical Research, Vol. 99, No. B12, 23,921–23,937.

[10] Dijkstra, H. A., Burgers, G., 2002, Fluid Dynamics of El Niño Variability, Annual review of fluid mechanics, Vol. 34, 531–558.

[11] Eubanks, T. M., Stepee, J. A., Dickey, J. O.: 1986, The El Niño, the Southern Oscillation and the Earth Rotation, in Earth Rotation: Solved and Unsolved Problems, edited by A. Cazenave, 163–186, D. Reidel Publishing Company, Dordrecht, Holland.

[12] Foster, M. R., Guinzy, N. J.: 1967, The coefficient of Coherence: Its estimation and use in Geophysical Data processing, Geophysics, Vol. XXXII, No. 4, 602–616.

[13] Gross, R. S.: 2000, The excitation of the Chandler Wobble, Geophysical Research Letters, Vol. 27, No. 15, 2329–2332.

[14] Groten, E., Fenoglio-marc, L., Wang, L.: 2000, El Niño (1997)-main characteristics and inter-annual earth rotation variability, Allgemeine Vermessungs-Nachrichten, Vol. 4, 140–146.

[15] Höpfner, J.: 1996, Seasonal oscillations in length of day, Astronomische Nachrichten, Vol. 317, No. 4, 273–280.

[16] Höpfner, J.: 2001, Atmospheric, Oceanic and hydrological contributions to seasonal variations in length of day, Journal of Geodesy, Volume 75, Nos. 2–3, 137–150.

[17] IRI: 2004 (reference year), El Niño and La Niña Events since 1950, http://iri. columbia.edu/climate/ENSO/background/pastevent.html, International Research Institute for Climate Prediction, USA.

[18] Jenkins, G. M., Watts, D. G.: 1968, Spectral analysis and its application, Holden-Day, San Francisco, U.S.A.

[19] Jochmann, H., Greiner-Mai, H.: 1996, Climate Variations and the Earths Rotation, Journal of Geodynamics, Vol. 21, No. 2, 161–176.

[20] Johnson, T. J., Wilson , C. R., Chao , B. F.: 1999, Oceanic angular momentum variability estimated from the Parallel Ocean Climate Model, 1988–1998, Journal of Geophysical Research , Vol. 104, 25183–25196.

[21] Latif, M., Anderson, D., Barnett, T., Cane, M., Kleeman, R., Letmaa, A., O'Brien, J., Rosati, A., Schneider, E.: 1998, A review of the predictability and prediction of ENSO, Journal of Geophysical Research, Vol. 103, No. C7, 14,375–14,393.

[22] McCarthy, D. D., Petit, G.: 2004, IERS Conventions, IERS Technical Note No. 32, Verlag des BKG, Frankfurt am Main, Germany.

[23] Otnes, R. K., Enochson, L.: 1972, Digital Time Series Analysis, John Wiley & Sons Inc., New York, U.S.A.

[24] Press, W. H., Teukolsky, S. A., Vetterling, W. T., Flannery, B. P.: 2002, Numerical recipes in C++, Cambridge University Press, UK.

[25] Rabiner, L. R., Gold, B.: 1975, Theory and Application of Digital Signal Processing. Englewood Cliffs, Prentice-Hall, New Jersey, USA.

[26] Rosen, R. D., Salstein, D. A., Eubanks, T. M., Dickey, J. O., Steppe, J. A.: 1984, An El Niño signal in atmospheric angular momentum and Earth rotation, Science, Vol. 225, No. 4660, 411–414.

[27] Stefanick, M.: 1982, Inter-annual atmospheric angular momentum variability 1963–1973 and Southern Oscillation, Journal of Geophysical Research, Vol. 87, No. C1., 428–432.

[28] Stockdale, T. N., Busalacchi, A. J., Harrison, D. E.: 1998, Ocean modeling for ENSO, Journal of Geophysical Research, Vol. 103., No. C7, Pgs 14,325–14,355.

[29] Suarez, M. J., Schopf, P. S.: 1988, A delay action oscillator for ENSO, Journal of the Atmospheric Sciences, Vol. 45, 3283–3287.
[30] Tang, Y., Kleeman, R.: 2002, A new strategy for assimilating SST data for ENSO prediction, Geophysical Research Letters, Vol. 29, No. 17, 1841, 22-1–22-4.
[31] Thompson, R. O. R. Y.: 1979, Coherence Significance Levels; Notes and Correspondence, Journal of the Atmospheric Sciences, Vol. 36, 2020–2021.
[32] Welch, P. D.: 1967, "The Use of Fast Fourier Transform for the Estimation of Power Spectra: A Method Based on Time Averaging Over Short, Modified Periodograms." IEEE Trans. Audio Electroacoust. Vol. AU-15, 70–73.
[33] Yan, X.-H., Zhou, Y, Pan, J. Zheng, D., Fang, M., Liao, X., He M.-X., Liu, W. T., Ding, X.: 2002, Pacific warm pool excitation, earth rotation and El Niño southern Oscillations, Geophysical Research Letters, Vol. 29, No. 21, 2031, 27-1–27-4.
[34] Zhang R.-H., Zebiak, S. E., Kleeman, R., Keenlyside, N.: 2003, A new intermediate coupled model for El Niño simulation and prediction, Geophysical Research Letters, Vol. 30, No. 19, 2012, OCE 5-1–OCE 5-4.

Address of the authors:
Dr.-Ing. Elias Lewi,
Institut für Physikalische Geodäsie, TU Darmstadt,
Petersenstr. 13, D-64287 Darmstadt
Prof.Dr.-Ing.mult. Erwin Groten,
Institut für Physikalische Geodäsie, TU Darmstadt,
Petersenstr. 13, D-64287 Darmstadt

Zusammenfassung

Zur Untersuchung der Zusammenhänge zwischen dem El Niño-Phänomen (ENSO-El Niño-/Southern Oscillation) und den Variationen der Erdrotation wurden in einem ersten Schritt Korrelation und komplexe Kohärenzfunktion zwischen den Anomalien der Meeresoberflächentemperatur (SSTA = Sea Surface Temperature Anomaly) und den Variation der Tageslänge (variation in LOD = Length of Day) untersucht. Statt, wie üblich, den ENSO-Index zu verwenden, wurden hier die Oberflächentemperatur und LOD-Daten direkt verwendet. Dies erfolgte bewusst, um sowohl räumliche wie zeitliche Variationen gleichzeitig zu erfassen. Während die Korrelationskoeffizienten erwartungsgemäß zahlenmäßig im Bereich vorausgegangener Studien liegen wird hier deutlich, dass die zeitlichen Verzögerungen stark ortsabhängig sind. Um die numerischen Ergebnisse der komplexen Kohärenzanalyse mit den im Zeitbereich beobachteten zeitlichen Verzögerungen vergleichen zu können, wurden ideale Phasenverzögerungen mit robusten Schätzern ausgeglichen. Dabei ergab sich erstens, dass aus den Daten des ENSO-Index in Darwin (Nordaustralien) und Tahiti alleine keine gesicherten Ergebnisse gewonnen werden können. Damit wurde eine unserer früher aufgestellten Hypothesen bestätigt. Zweitens wurden weitergehende und vertiefte Erkenntnisse über die zeitlichen und regionalen Zusammenhänge zwischen Erdrotation (LOD) und dem ENSO-Phänomen gewonnen.

Abstract

As a first step toward establishing the interdependence between El Niño-/Southern Oscillation and changes in the Earth rotation parameters the correlation and complex coherence functions between the sea surface temperature and the variation in the length of day have been investigated. The investigation is made by directly correlating the sea surface temperature anomaly with variations in the Length of day, in contrary to the common practice of using the Southern Oscillation Index. This is done deliberately to analyze both the spatial and time dependence of the correlation. It has been found that the correlation coefficients have similar magnitudes to previous investigations that make use of the Southern Oscillation Index. The computation of the time lag, however, showed that it is location dependent. A robust estimation technique has been used to compute the time lag from the phase of the coherence function. The method implemented has given a remarkable result that has aided the interpretational procedure. The study also confirmed the initial assumption we had that the time lag cannot be entirely studied from the southern oscillation index only, which is computed using data from Darwin and Tahiti only.